Supporting Information

Coligand-directed structural and magnetic diversities in anisotropic Co^{II}-triazolate system

En-Cui Yang*, Zhong-Yi Liu, Tian-Yu Liu, Li-Ly Li, and Xiao-Jun Zhao*

Table S1 Selected Hydrogen Bond Lengths (Å) and Angles (°) [a]

D–H···A	*d* (D–H)	*d* (H···A)	*d* (D···A)	∠DHA
2				
O7–H7A···O2$^{\#1}$	0.85	2.00	2.813(6)	161
O7–H7B···O4$^{\#2}$	0.85	2.13	2.824(7)	138
O3–H3···O7$^{\#2}$	0.82	2.03	2.793(9)	155
N4–H4A···O7$^{\#3}$	0.86	2.18	3.002(6)	161
3				
N9–H9'···O4$^{\#1}$	0.90	2.30	2.926(1)	126

[a] Symmetry codes for **2** $^{\#1}$ $x - 1/2, 1/2 - y, z - 1/4$, $^{\#2}$ $1 - x, 1 - y, 1/2 - z$, $^{\#3}$ $x - 1, y, - z$; for **3** $^{\#1}$ $- x, 1 - y, 2 - z$.

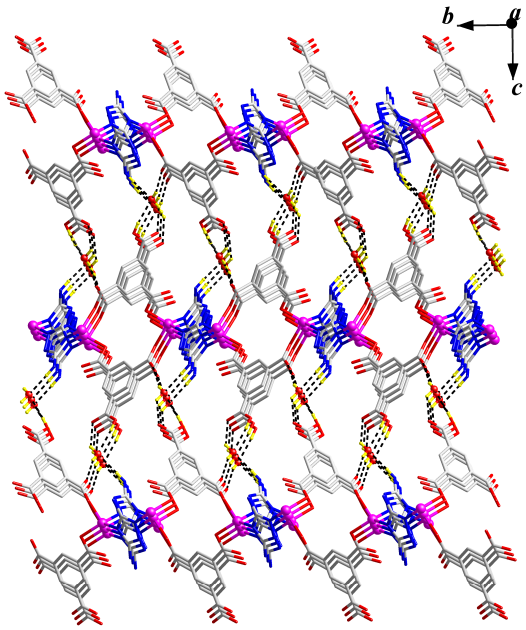

Fig. S1 3D supramolecular network of **2** by hydrogen-bonding interactions.

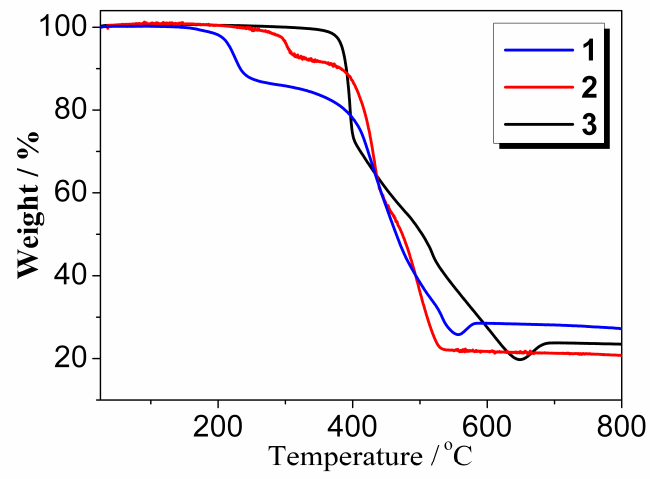

Fig. S2 TG curves for complexes **1** – **3**.

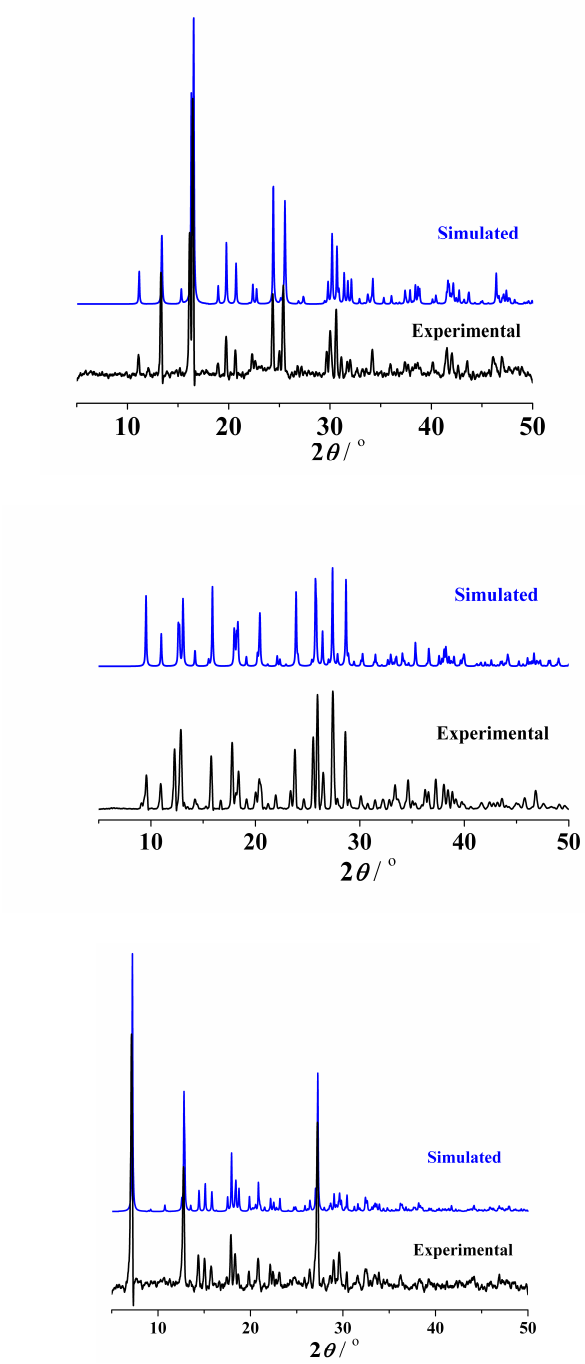

Fig. S3. Simulated (blue) and experimental (black) X-ray powder diffraction patterns for **1 – 3**.

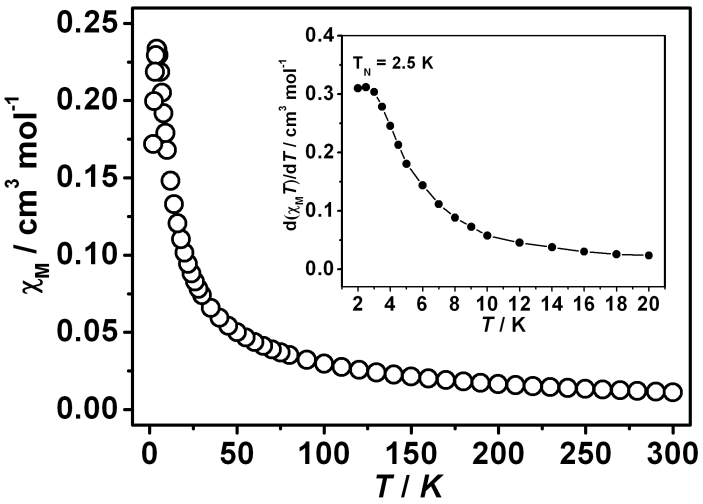

Fig S4. Plot of χ_M *vs. T* for **1** (Inset: the d$\chi_M T$/dT curve at low temperature).

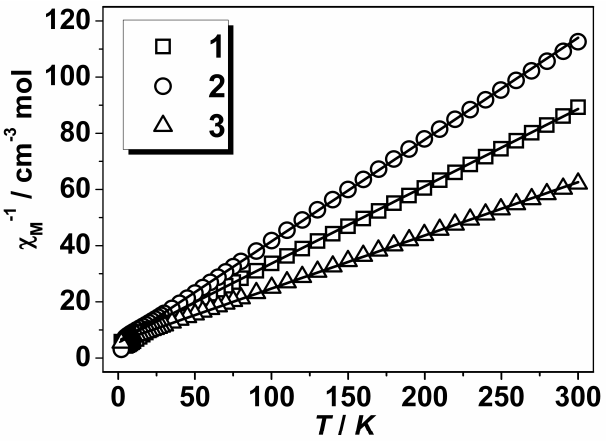

Fig S5. Temperature dependence of χ_M^{-1} for **1 – 3** (The solid lines represent the best fit to Curie-Weiss law).

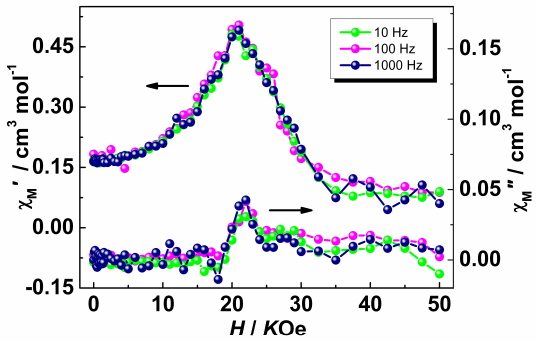

Fig S6. Field-dependent ac magnetic susceptibilities of **1** measured in an ac field of 3.5 Oe at various frequencies.